

# Methane and Climate



# **Methane and Climate**

**W.A. van Wijngaarden**

**W. Happer**

**January 2025**

## TABLE OF CONTENTS

Abstract .....	3
Introduction .....	3
The Methane Molecule .....	4
Greenhouse Gases in the Atmosphere .....	5
Fluxes and Forcings .....	7
Spectral Forcings .....	8
Temperature Changes Caused by Forcing Changes .....	12
Future Forcing from CH <sub>4</sub> and CO <sub>2</sub> .....	14
Acknowledgments .....	18
References .....	20

## ABSTRACT

Atmospheric methane ( $\text{CH}_4$ ) contributes to the *radiative forcing* of Earth's atmosphere. Radiative forcing is the difference in the net upward thermal radiation from the Earth through a transparent atmosphere and radiation through an otherwise identical atmosphere with greenhouse gases. Radiative forcing, normally specified in units of  $\text{W m}^{-2}$ , depends on latitude, longitude and altitude, but it is often quoted for a representative temperate latitude, and for the altitude of the tropopause, or for the top of the atmosphere. For current concentrations of greenhouse gases, the radiative forcing at the tropopause, per added  $\text{CH}_4$  molecule, is about 30 times larger than the forcing per added carbon-dioxide ( $\text{CO}_2$ ) molecule. This is due to the heavy saturation of the absorption band of the abundant greenhouse gas,  $\text{CO}_2$ . But the rate of increase of  $\text{CO}_2$  molecules, about 2.3 ppm/year (ppm = part per million), is about 300 times larger than the rate of increase of  $\text{CH}_4$  molecules, which has been around 0.0076 ppm/year since the year 2008. So, the contribution of methane to the annual increase in forcing is one tenth (30/300) that of carbon dioxide. The net forcing increase from  $\text{CH}_4$  and  $\text{CO}_2$  increases is about  $0.05 \text{ W m}^{-2} \text{ year}^{-1}$ . Other things being equal, this will cause a temperature increase of about  $0.011 \text{ }^\circ\text{C year}^{-1}$ . Proposals to place harsh restrictions on methane emissions because of warming fears are not justified by facts.

## INTRODUCTION

This is a summary of a more detailed paper on radiative forcing by greenhouse gases that we will refer to as "WH" [1]. We assume most readers of this paper will have little background in quantitative sciences, but since much of the concern over climate change and greenhouse gases comes from misunderstanding basic physics, we have included a few fundamental equations. We explain the physical meaning of all equations in plain English for readers with little quantitative background.

The paper is focused on the greenhouse effects of atmospheric methane, since there have recently been proposals to put harsh restrictions on any human activities that release methane. The basic radiation-transfer physics outlined in this paper gives no support to the idea that greenhouse gases like methane,  $\text{CH}_4$ , carbon dioxide,  $\text{CO}_2$  or nitrous oxide,  $\text{N}_2\text{O}$ , are contributing to a climate crisis. Given the huge benefits of more  $\text{CO}_2$  to agriculture, to forestry and to primary photosynthetic productivity in general, more  $\text{CO}_2$  is almost certainly benefitting the world. Radiative effects of  $\text{CH}_4$  and  $\text{N}_2\text{O}$ , another greenhouse gas produced by human activities, are so small that they are irrelevant to climate.

## THE METHANE MOLECULE

Methane,  $\text{CH}_4$ , is the simplest *hydrocarbon* molecule. It has a single carbon atom, C, bonded to four hydrogen atoms, H, as sketched in Fig. 1. Natural-gas is mostly methane [2]. Large amounts of methane are found in some coal seams [3]. Methane is produced by the anaerobic decomposition of organic matter as marsh gas [4], and huge amounts of methane can be found as methane clathrates [5] in seafloor sediments, the Arctic tundra and other locations on Earth. Large amounts of methane are produced in the digestive tracts of ruminants, like cattle and sheep, where symbiotic, anaerobic bacteria convert some of the cellulose of plant material to nutritionally useful fatty acids and other compounds [6], with methane as a byproduct. Similarly, bacteria in the digestive tracts of termites also produce large amounts of methane [7]. Methane has a half-life of about 10 years in the atmosphere, before it is oxidized to carbon dioxide and water [8].

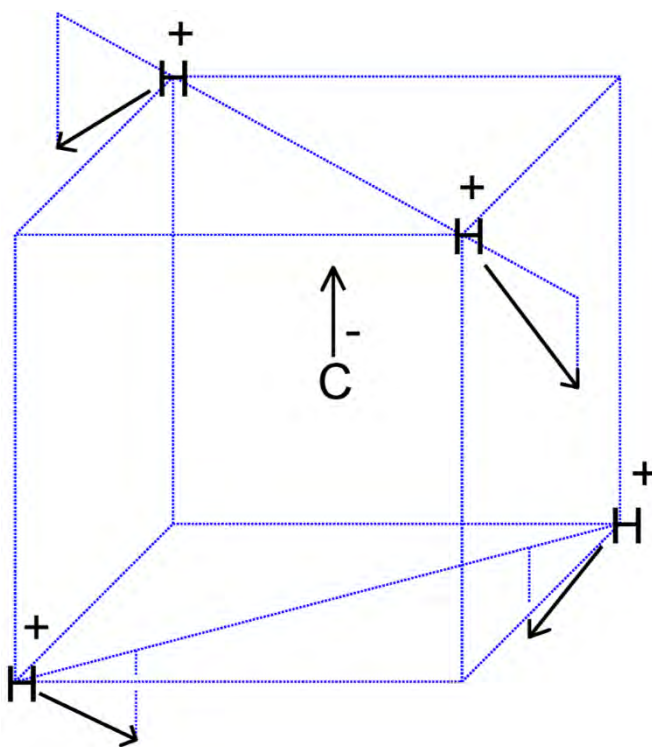


**Figure 1:** *Geometry of a methane molecule,  $\text{CH}_4$ . The four hydrogen atoms H are centered at the corners of a cube and the carbon atom, C, is at the center. Near the H atoms the molecule has a slightly positive electrical charge, and near the central carbon atom the molecule has a slightly negative charge. Also shown is a representative asymmetric bending vibration of the molecule, which dominates the greenhouse forcing. The carbon atom moves up while the top two hydrogen atoms bend outward, and the bottom two hydrogen atoms bend inward. The accelerating charges emit radiation with a spatial frequency of  $1,306 \text{ cm}^{-1}$  (waves per cm). Thermally excited molecular rotations spread the emission frequencies from about  $1,200 \text{ cm}^{-1}$  to  $1,400 \text{ cm}^{-1}$ .*

## GREENHOUSE GASES IN THE ATMOSPHERE

Radiation transfer in the cloud-free atmosphere of the Earth is controlled by only two factors: (1) the temperature  $T = T(z)$  at the altitude  $z$ , and (2) the number densities,  $N^{(i)} = N^{(i)}(z)$  of the  $i$ th type of greenhouse gas molecule. Although the altitude profiles of temperature and number densities vary with latitude and longitude, the horizontal variation is normally small enough to neglect when calculating local radiative forcing. The dependence of the temperature on altitude is as important as the concentration of greenhouse gases. If the temperature were the same from the surface to the top of the atmosphere, there would be no radiative forcing, no matter how high the concentration of greenhouse gases.

Representative midlatitude altitude profiles of temperature [9], and concentrations of greenhouse gases [10], are shown in Fig. 2. Altitude profiles directly measured by radiosondes in ascending balloons [11] are always much more complicated than those of Fig. 2, which can be thought of as time-averaged profiles. Collision rates of molecules in the Earth's troposphere and stratosphere are sufficiently fast that a single local temperature  $T = T(z)$  provides an excellent description of the distribution of molecules between translational, vibrational and rotational energy levels. However, radiation in the atmosphere is almost never in full thermal equilibrium because at many frequencies, the mean-free paths of photons can exceed the atmospheric thickness.

On the left of Fig. 2 we have indicated the three most important atmospheric layers for radiative heat transfer. The lowest atmospheric layer is the troposphere, where parcels of air, warmed by contact with the solar-heated surface, float upward, much like hot-air balloons. As they expand into the surrounding air, the parcels do work at the expense of internal thermal energy. This causes the parcels to cool with increasing altitude, since heat flow in or out of parcels is usually slow compared to the velocities of ascent or descent. If the parcels consisted of dry air, the cooling rate would be  $9.8 \text{ }^\circ\text{C km}^{-1}$  the *dry adiabatic lapse rate* [12]. But rising air has usually picked up water vapor from the land or ocean, and the condensation of water vapor to droplets of liquid or to ice crystallites in clouds, releases so much latent heat that the lapse rates are less than  $9.8 \text{ }^\circ\text{C km}^{-1}$  in the lower troposphere. A representative lapse rate for midlatitudes is  $-dT/dz = 6.5 \text{ K km}^{-1}$  as shown in Fig. 2. The tropospheric lapse rate is familiar to vacationers who leave hot areas near sea level for cool vacation homes at higher altitudes in the mountains. On average, the temperature lapse rates are small enough to keep the troposphere buoyantly stable [13] so that higher-altitude cold air does not sink to replace lower-altitude warm air. Tropospheric air parcels that are displaced in altitude will oscillate up and down with periods of a few minutes. However, at any given time, large regions of the troposphere (particularly in the tropics) are unstable to moist convection because of exceptionally large temperature lapse rates.

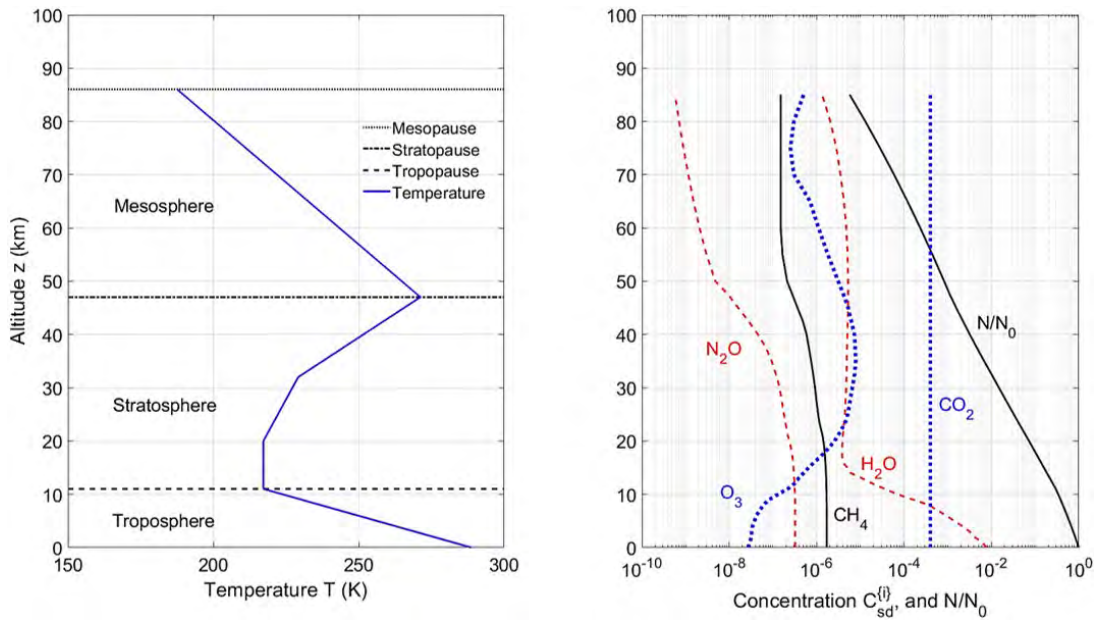


**Figure 2: Left.** A standard atmospheric temperature profile [9],  $T = T(z)$ . The surface temperature is  $T(0) = 288.7$  K. **Right.** Standard concentrations [10],  $C_{sd}^{(i)} = N_{sd}^{(i)}/N$  for greenhouse molecules versus altitude  $z$  ( $N = N_0$  at the Earth's surface). The total number density of atmospheric molecules is  $N$  and the number density of molecules of type  $i$  is  $N_{sd}^{(i)}$ . At sea level the concentrations are 7,750 ppm of  $H_2O$ , 1.8 ppm of  $CH_4$  and 0.32 ppm of  $N_2O$ . The  $O_3$  concentration peaks at 7.8 ppm at an altitude of 35 km, and the  $CO_2$  concentration was approximated by 400 ppm at all altitudes. The data is based on experimental observations.

Above the troposphere is the stratosphere, which extends from the tropopause to the stratopause, at a typical altitude of  $z_{sp} = 47$  km, as shown in Fig. 2. Stratospheric air is much more stable to vertical displacements than tropospheric air, and negligible moist convection occurs there. For midlatitudes, the temperature of the lower stratosphere is nearly constant, at about 220 K, but it increases at higher altitudes, reaching a peak temperature not much less than the surface temperature at the stratopause. The stratospheric heating is due to the absorption of solar ultraviolet radiation by ozone molecules,  $O_3$ . The average solar flux at the top of the atmosphere is about 1,350 Watts per square meter ( $W m^{-2}$ ) [14]. Approximately 9% consists of ultraviolet light (with wavelengths shorter than  $\lambda = 405$  nanometers (nm)) which can be absorbed in the upper atmosphere.

Above the stratosphere is the mesosphere, which extends from the stratopause to the mesopause at an altitude of about  $z_{mp} = 86$  km. With increasing altitudes, radiative cooling, mainly by  $CO_2$ , becomes increasingly more important compared to heating by solar ultraviolet radiation. This causes the temperature to decrease with increasing altitude in the mesosphere.

Above the mesopause, is the extremely low-pressure thermosphere, where convective mixing processes are negligible. Temperatures increase rapidly with altitude in the thermosphere, to as high as 1,000 K, due to heating by extreme ultraviolet sunlight, the solar wind and atmospheric waves. Polyatomic gases break up into individual atoms, and there is gravitational stratification, with lighter gases increasingly dominating at higher altitudes.

The vertical radiation flux  $Z$ , which is discussed below, can change rapidly in the troposphere and stratosphere. There can be a further small change of  $Z$  in the mesosphere. Changes in  $Z$  above the mesopause are small enough to be neglected, so we will often refer to the mesopause as “the top of the atmosphere” (TOA), with respect to radiation transfer.

As shown in Fig. 2, the most abundant greenhouse gas at the surface is water vapor. However, the concentration of water vapor drops by a factor of a thousand or more between the surface and the tropopause. This is because of condensation of water vapor into clouds and eventual removal by precipitation.

Carbon dioxide,  $\text{CO}_2$ , the most abundant greenhouse gas after water vapor, is also the most uniformly mixed because of its chemical stability.

Methane, the main topic of this discussion, is much less abundant than  $\text{CO}_2$  and its concentration decreases somewhat in the stratosphere because of oxidation by OH radicals and ozone,  $\text{O}_3$ . The oxidation of methane [8] is a major source of the stratospheric water vapor shown in Fig. 2.

Ozone molecules,  $\text{O}_3$ , are produced from  $\text{O}_2$  molecules by ultraviolet sunlight in the upper atmosphere, and this is the reason that  $\text{O}_3$  concentrations peak in the stratosphere, and are hundreds of times smaller in the troposphere, as shown in Fig. 2.

## FLUXES AND FORCINGS

How greenhouse gases affect energy transfer through Earth’s atmosphere is quantitatively determined by the *radiative forcing*,  $F$ , the difference between the flux  $\sigma T_0^4$  of thermal radiant energy from a black surface through a hypothetical, transparent atmosphere, and the flux  $Z$  through an atmosphere with greenhouse gases, particulates and clouds, but with the same surface temperature,  $T_0$  [15],

$$F = \sigma T_0^4 - Z. \quad (1)$$

Here the Stefan-Boltzmann constant is

$$\sigma = 5.67 \times 10^{-8} \text{ W m}^{-2} \text{ K}^{-4} \quad (2)$$



The forcing  $F$  and the flux  $Z$  are usually specified in units of  $\text{W m}^{-2}$ . The radiative heating rate,

$$R = dF/dz, \quad (3)$$

is equal to the rate of change of the forcing with increasing altitude  $z$ . Over most of the atmosphere,  $R < 0$ , so thermal infrared radiation is a cooling mechanism that transfers internal energy of atmospheric molecules to space or to the Earth's surface. Forcing depends on latitude, longitude and on the altitude,  $z$ . The right panel of Fig. 3 shows the altitude dependence of the net upward flux  $Z$  and the forcing  $F$  for the greenhouse gas concentrations of Fig. 2. The temperature profile of Fig. 2 is reproduced in the left panel. The altitude-independent flux,  $\sigma T_0^4 = 394 \text{ W m}^{-2}$ , from the surface with a temperature  $T_0 = 288.7 \text{ K}$ , through a hypothetical transparent atmosphere, is shown as the vertical dashed line in the panel on the right. The fluxes for current concentrations of  $\text{CO}_2$  and for doubled or halved concentrations are shown as the continuous green line, the dashed red line and the dotted blue line, respectively.

At current greenhouse gas concentrations, the surface flux,  $142 \text{ W m}^{-2}$ , is less than half the surface flux of  $394 \text{ W m}^{-2}$  for a transparent atmosphere because of downwelling radiation from greenhouse gases above. The flux has nearly doubled to  $257 \text{ W m}^{-2}$  at the tropopause altitude, 11 km in this example. The  $115 \text{ W m}^{-2}$  increase in flux from the surface to the tropopause has been radiated by greenhouse gases in the troposphere. Most of the energy needed to replace the radiated power comes from convection of moist air. Direct absorption of sunlight in the troposphere makes a much smaller contribution.

From Fig. 3 we see that the flux  $Z$  increases by another  $20 \text{ W m}^{-2}$ , from  $257 \text{ W m}^{-2}$  to  $277 \text{ W m}^{-2}$  between the tropopause and the top of the atmosphere. The energy needed to replace the  $20 \text{ W m}^{-2}$  increase in flux comes from the absorption of solar ultraviolet light by ozone,  $\text{O}_3$ , in the stratosphere and mesosphere. Convective heat transport above the tropopause is small enough to be neglected.

## SPECTRAL FORCINGS

In Eq. (1), the fluxes,  $Z$ , and forcings,  $F$ , of Fig. 3 can be thought of as sums of contributions,  $\tilde{Z}dv$  and  $\tilde{F}dv$ , from *spectral fluxes*,  $\tilde{Z}$ , or *spectral forcings*,  $\tilde{F}$ , carried by infrared radiation of spatial frequencies between  $\nu$  and  $\nu + dv$ . As one can see from Fig. 3, at the top of the atmosphere, the sums (integrals) of the spectral fluxes and spectral forcings are

$$Z = \int_0^{\infty} \tilde{Z} dv = 277 \text{ W m}^{-2}, \quad (4)$$

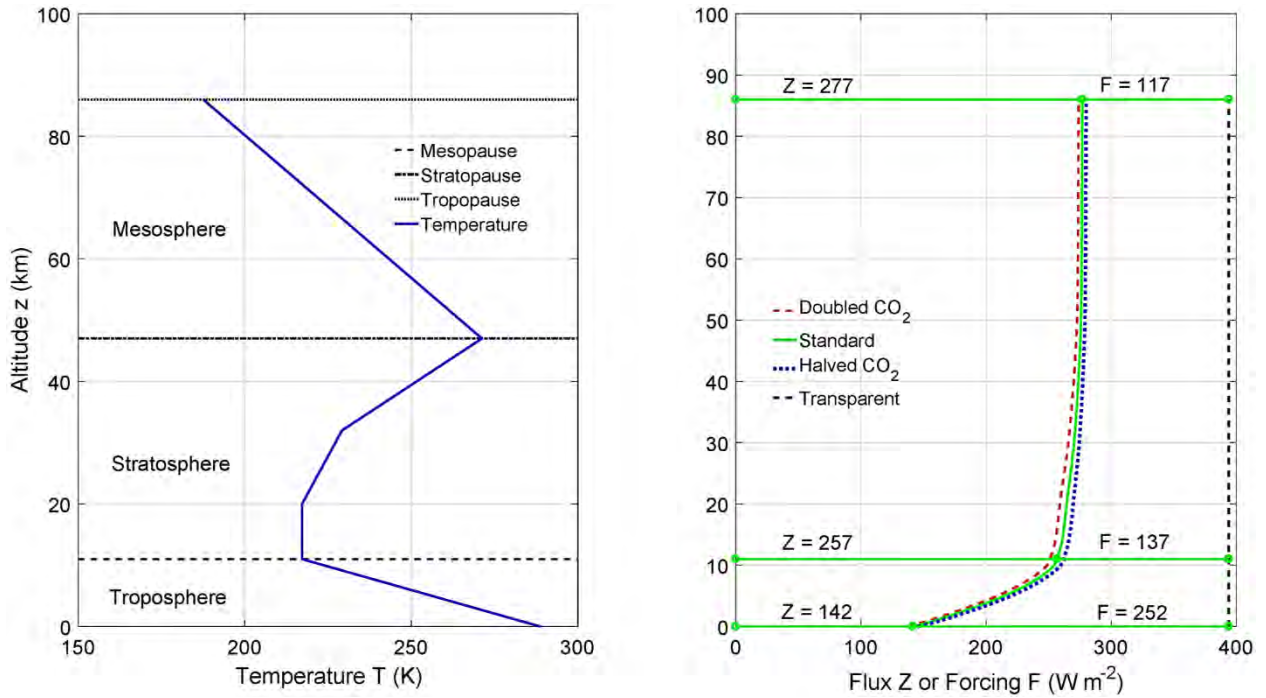


**Figure 3:** *Left:* The altitude dependence of temperature from Fig. 2. *Right:* The flux  $Z$  increases with increasing altitude as a result of net upward energy radiation from the greenhouse gases  $H_2O$ ,  $O_3$ ,  $N_2O$  and  $CH_4$ , and  $CO_2$ . The middle, green curve is the flux for 2020 concentrations. The forcings  $F$  are the differences between the altitude-independent flux  $\sigma T_0^4 = 394 \text{ W m}^{-2}$  (the vertical, dashed black line) through a transparent atmosphere with no greenhouse gases, for a surface temperature of  $T_0 = 288.7 \text{ K}$ , and the flux  $Z$  for an atmosphere with the greenhouse gas concentrations of Fig. 2. Fluxes and forcings for halved and doubled concentrations of  $CO_2$ , but with the same concentrations of all other greenhouse gases, are shown as dotted blue and dashed red curves, which barely differ from the green curve, the flux for current concentrations. We used doubled and halved  $CO_2$  rather than  $CH_4$  for this illustration since the flux changes for doubling or halving methane concentrations would be ten times smaller and would not be distinguishable on the figure.

and

$$F = \int_0^{\infty} \tilde{F} \, d\nu = 117 \text{ W m}^{-2}. \quad (5)$$

Representative spectral fluxes and forcings are plotted in Figures 4 and 5. The integral (4) is the area under the jagged black curve. The spectral fluxes and forcings are related by a formula analogous to (1)

$$\tilde{F} = \pi \tilde{B}_0 - \tilde{Z}. \quad (6)$$

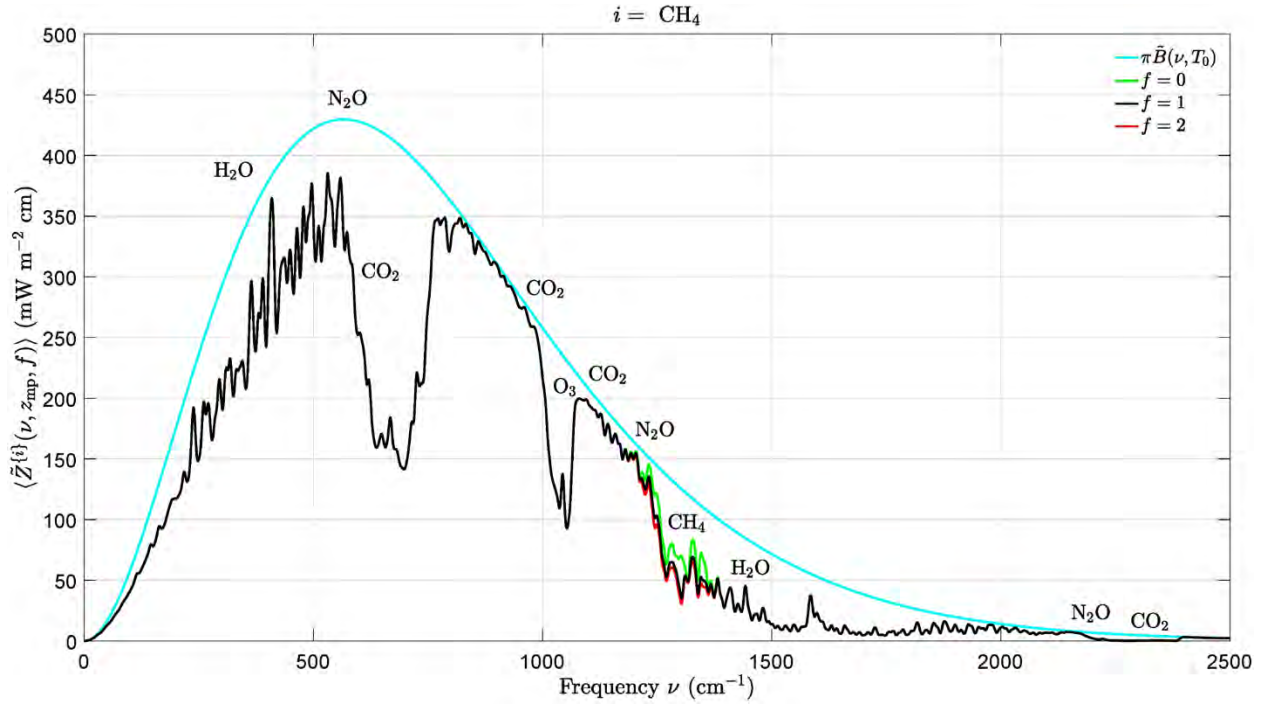


**Figure 4:** The spectral forcing at current levels of methane,  $\text{CH}_4$ , (the black curve with  $f = 1$ ), or if concentrations of methane are doubled from 1.8 to 3.6 ppm (the red curve with  $f = 2$ ), or if all methane is removed (the green curve with  $f = 0$ ). The area under the black, jagged curve is  $227 \text{ W m}^{-2}$  and is the frequency-integrated flux at the top of the atmosphere of Fig. 3. The area under the Planck spectral intensity (the smooth cyan curve) is  $394 \text{ W m}^{-2}$ . It is the flux,  $\sigma T_0^4$ , that would be radiated to space by a black surface at the temperature  $T_0 = 288.7 \text{ K}$  for an atmosphere that contained no greenhouse gases and was transparent to thermal radiation.

Here  $\tilde{B}_0 = \tilde{B}(\nu, T_0)$ , is the surface value of the spectral Planck intensity,

$$\tilde{B} = \frac{2h_{\text{PC}}^2 \nu^3}{e^{h_{\text{PC}} \nu / (k_{\text{B}} T_0)} - 1}, \quad (7)$$

which depends on the spatial frequency  $\nu$  and the temperature  $T$  of the radiation. In (7), Boltzmann's constant is  $k_{\text{B}} = 1.3806 \times 10^{-16} \text{ erg K}^{-1}$ , Planck's constant is  $h_{\text{P}} = 6.6261 \times 10^{-27} \text{ erg s}$ , and the speed of light,  $c = 2.9979 \times 10^{10} \text{ cm s}^{-1}$ . The spatial frequency of the radiation,  $\nu = 1/\lambda$ , is the inverse of the wavelength  $\lambda$  of the radiation. Versions of (6) with wavelength  $\lambda$  or temporal frequency ( $c\nu \rightarrow \nu$ ) are often given in the literature [16]. The spatial frequency  $\nu$  is usually given in units of  $\text{cm}^{-1}$ . The spectral flux from the "black" surface of a hypothetical transparent atmosphere is  $\pi \tilde{B}_0$ , where the factor of  $\pi$  comes from integrating  $\tilde{B}_0 \cos \theta$  over  $2\pi$  steradians of solid angle, in accordance with a Lambertian [17] angular dependence.

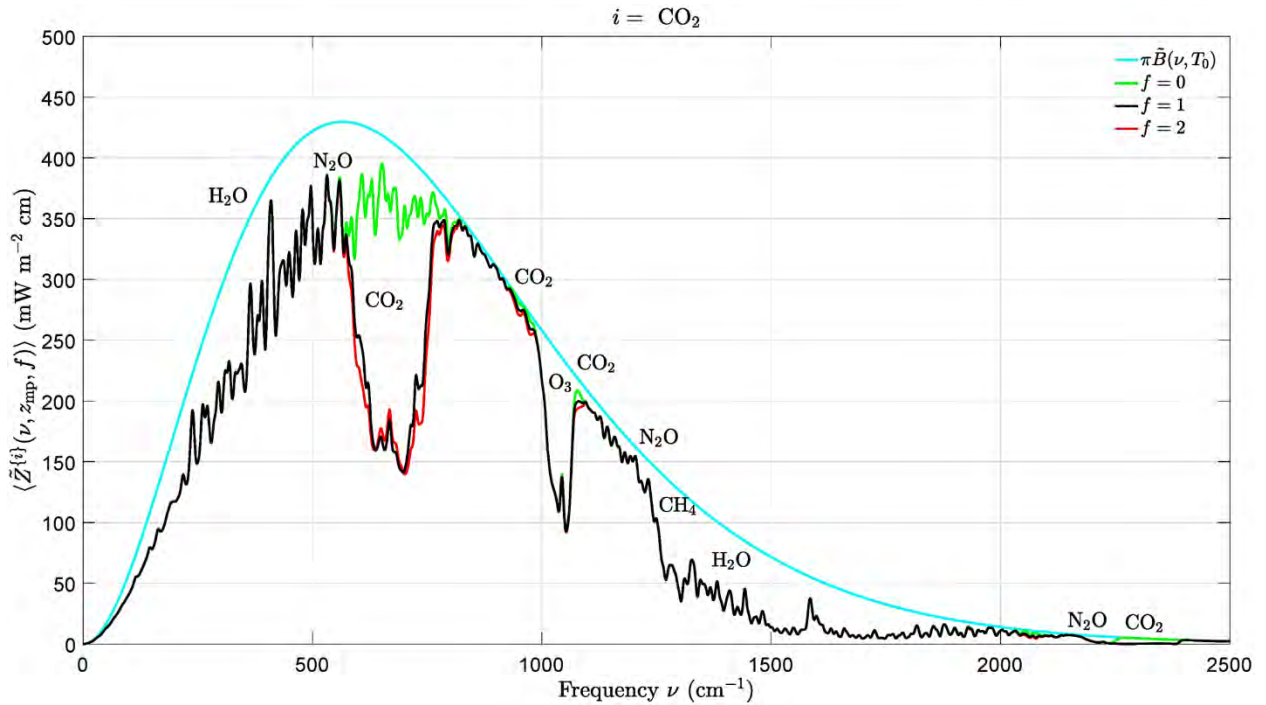


**Figure 5:** The spectral forcing at current levels of carbon dioxide,  $\text{CO}_2$ , (the black curve with  $f = 1$ ), or if concentrations of carbon dioxide are doubled from 400 to 800 ppm (the red curve with  $f = 2$ ), or if all carbon dioxide is removed (the green curve with  $f = 0$ ). See the caption of Fig. 4.

Planck's spectral intensity (7) is one of the most famous equations of physics. It finally solved the classical problem of heat radiation, and it gave birth to quantum mechanics [16].

The Stefan-Boltzman flux,  $\sigma T_0^4 = 394 \text{ W m}^{-2}$  of (1), for a surface temperature of  $T_0 = 288.7 \text{ K}$ , is the frequency integral of the Planck spectral flux,  $\pi \tilde{B}_0$ ,

$$\int_0^{\infty} \pi \tilde{B}_0 d\nu = \sigma T_0^4 = 394 \text{ W m}^{-2}. \quad (8)$$

The integral (8) is the area in Fig. 4 beneath the smooth blue curve, the spectral flux for a transparent atmosphere.

As one can see from Fig. 3, the flux at the top of the atmosphere,  $277 \text{ W m}^{-2}$  is only 70.3% of the flux  $\sigma T_0^2 = 394 \text{ W m}^{-2}$  emitted by a black surface at a temperature of  $T_0 = 288.7 \text{ K}$ . So without greenhouse gases, the surface would only need to radiate 70.3% of its current value to balance the same amount of solar heating. Since the Stefan-Boltzman flux is proportional to the fourth power of the surface temperature, without greenhouse gases the surface temperature could be smaller by a factor of  $(0.703)^{1/4} = 0.916$ . So for this highly simplified example, the greenhouse warming of the surface by all the

greenhouse gases of Fig. 2 is  $\Delta T = (1 - 0.916)T_0 = 24.3$  K. This number would be different at different latitudes and longitudes, or in summer or winter, or if clouds are taken into account. But 20 °C to 30 °C is a reasonable estimate of how much warming is caused by current concentrations of greenhouse gases, compared to a completely transparent atmosphere.

## TEMPERATURE CHANGES CAUSED BY FORCING CHANGES

Instantaneous forcing increments, due to changes in the concentrations of greenhouse gases, can be calculated accurately. The next step, using instantaneous forcing increments to calculate temperature changes, is fraught with difficulties and is a major reason that climate models predict much more warming than observed [18]. As shown in Fig. 3, increasing the concentration of greenhouse gases (doubling the CO<sub>2</sub> concentration for the example in the figure) slightly decreases the radiation flux through the atmosphere. In response, the atmosphere will slightly change its properties to ensure that the average energy absorbed from sunlight is returned to space as thermal radiation. Since both the surface and greenhouse molecules radiate more intensely at higher temperatures, temperature increases are an obvious way to restore the equality of incoming and outgoing energy. But the amount of water vapor and clouds in the atmosphere will also change, since water vapor is evaporated from the oceans and from moist land. Water is also precipitated from clouds as condensed rain or snow. Low warm clouds reflect more sunlight and reduce solar heating, with little hindrance of thermal radiation to space. High, cold cirrus clouds reduce the thermal radiation to space but are wispy and do little to hinder solar heating of the Earth.

The simplest response to changes in radiative forcing would be a uniform temperature increase  $dT$ , at every altitude and at the surface. The rate of increase of top-of-the-atmosphere flux with a uniform temperature increment is [1]

$$dZ/dT = 3.9 \text{ W m}^{-2} \text{ K}^{-1}. \quad (9)$$

For a uniform temperature increase, the forcing increase  $\Delta F = 0.23 \text{ W m}^{-2}$  after 50 years, that would result if methane concentrations continued to rise at the rate of the previous 10 years as shown in Fig. 9, would cause a surface-temperature increase of  $\Delta T = \Delta F / (dZ/dT) = 0.05$  °C. The forcing increase  $\Delta F = 2.2 \text{ W m}^{-2}$  after 50 years, if carbon-dioxide concentrations continued to rise at the rate of the previous 10 years, would cause a surface-temperature increase of  $\Delta T = \Delta F / (dZ/dT) = 0.57$  °C.

But there are persuasive reasons to expect that the temperature changes will be altitude dependent, like the forcing changes shown in Fig. 3, and that the water-vapor concentrations and cloud cover will change in response to changes in the surface temperature. Fig. 6 illustrates a more complicated “feedback” calculation. On the left

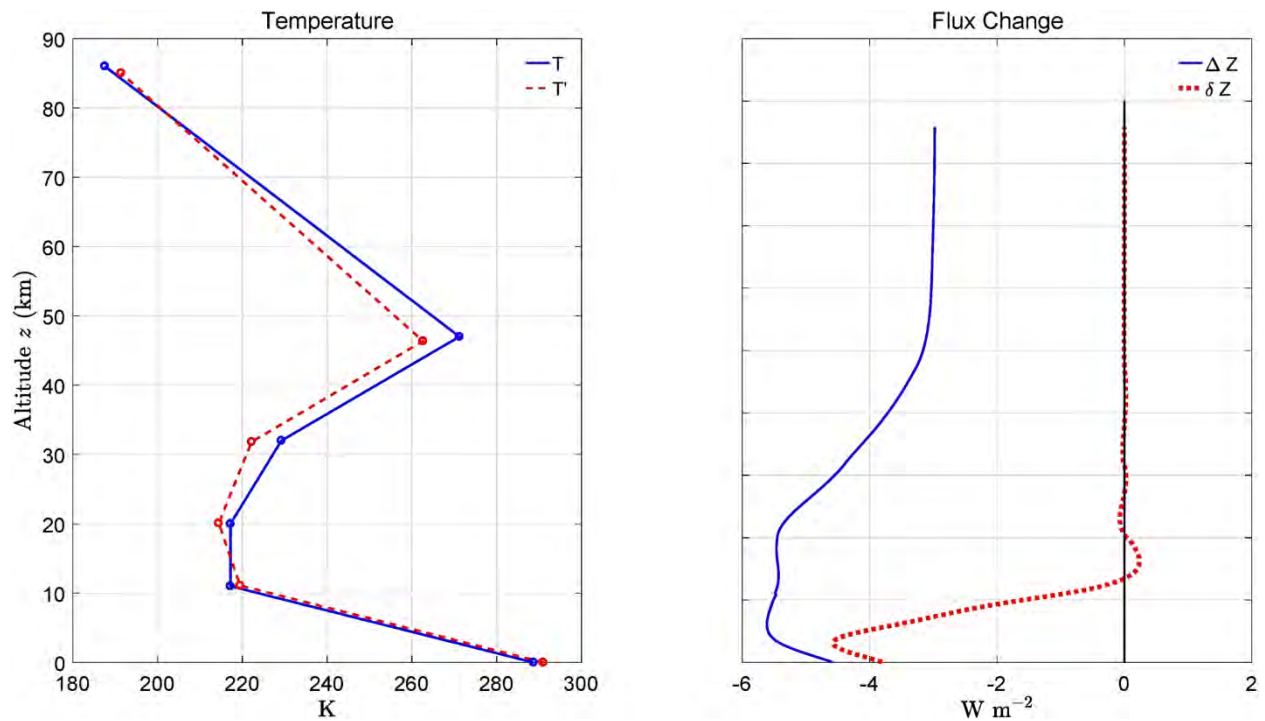


**Figure 6:** *Left.* An initial temperature profile  $T$  (continuous blue line), the midlatitude profile of Fig. 3. The dashed red line is the adjusted temperature profile  $T'$ , after a doubling of the  $\text{CO}_2$  concentration. *Right.* The continuous blue line is the altitude profile of the “instantaneous” flux change  $\Delta Z$ , caused by doubling  $\text{CO}_2$  concentrations. The concentrations of all other greenhouse gases, and the temperature profile are held fixed for the blue line. The dashed red curve  $\delta Z$  on the right of this Figure is the difference between the initial flux and the flux for doubled concentrations of  $\text{CO}_2$  and for the adjusted temperature profile  $T'$  on the left of the figure. See the text for more details of the adjustments.

panel of Fig. 6, the continuous blue line labeled  $T$  is the midlatitude temperature profile of Fig. 3. The dashed red line labeled  $T'$  is the adjustment of the temperature profile in response to doubling the concentration of  $\text{CO}_2$ , with a simultaneous increase in the concentration of water vapor in the troposphere. The right panel of Fig. 6 summarizes forcing increments, with and without feedbacks. The continuous blue line is the instantaneous flux change from doubling  $\text{CO}_2$  concentrations, with no other changes to the atmosphere. It is the difference between the dashed red curve and the continuous green curve on the right of Fig. 3, but plotted on an expanded scale. The instantaneous forcing,  $\Delta F = -\Delta Z$ , is  $5.5 \text{ W m}^{-2}$  at the tropopause altitude of 11 km, and  $3.0 \text{ W m}^{-2}$  at the 86 km altitude of the top of the atmosphere. The dashed red curve on the right of Fig. 6, labeled  $\delta Z$  is the “residual forcing” for the dashed-red temperature profile  $T'$  on the left, for doubled  $\text{CO}_2$  concentrations, and for the same relative humidity as before doubling  $\text{CO}_2$ . The same lapse rate,  $dT/dz = 6.5 \text{ K km}^{-1}$ , was used before and after doubling  $\text{CO}_2$

concentrations, as proposed by Manabe and Wetherald [19] in their model of “radiative-convective equilibrium.” This feedback increases the surface warming by a factor of about 1.6, compared to a uniform temperature adjustment and no change in water-vapor concentration. It leads to stratospheric cooling and surface warming. Variants of the radiative-convective equilibrium recipes illustrated in Fig. 6 are widely used in climate models. Unlike forcing calculations, which can be uniquely and reliably calculated, there is lots of room for subjective adjustments of the temperature changes caused by forcing changes.

## FUTURE FORCING FROM CH<sub>4</sub> AND CO<sub>2</sub>

Methane levels in Earth’s atmosphere are slowly increasing, as shown in Fig. 7. If the current rate of increase, about 0.0076 ppm/year, were to continue unchanged, it would take about 270 years to double the 2020 concentration of  $C^{(i)} = 1.8$  ppm. But as one can see from Fig. 7, methane levels have stopped increasing for years at a time (for example, between 2000 and 2008) so it is hard to be confident about future concentrations. Methane concentrations may never double, but if they do, WH[1] show that this would only increase the forcing by  $0.8 \text{ W m}^{-2}$ . This is a tiny fraction of representative total forcings at midlatitudes of about  $140 \text{ W m}^{-2}$  at the tropopause and  $120 \text{ W m}^{-2}$  at the top of the atmosphere.

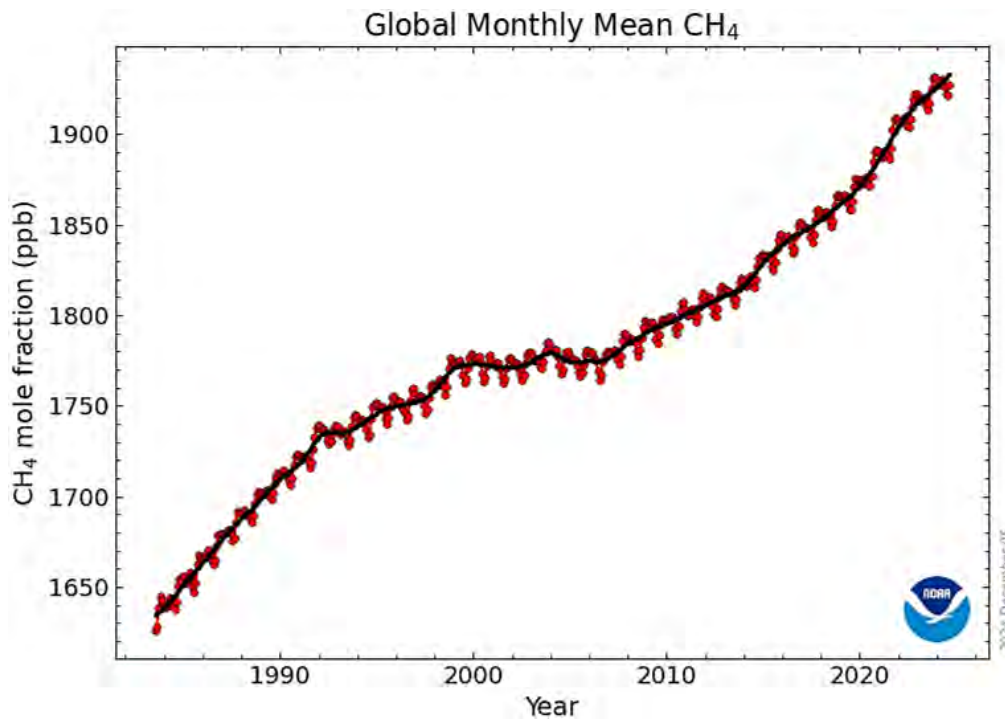


**Figure 7:** Atmospheric concentrations  $\bar{C}^{(i)}$  of methane molecules ( $i = \text{CH}_4$ ) versus time [8]. For the past 10 years, the average rate of increase has been about  $d\bar{C}^{(i)}/dt = 0.0076$  ppm/year.

Carbon dioxide levels in the atmosphere have been steadily increasing over the past half century and at a much faster rate than those of methane. Thanks to pioneering work by Charles Keeling [21], there are a number of observatories at various latitudes around the Earth, from the South Pole to the Arctic, that provide measurements of CO<sub>2</sub> like those of Fig. 8. In WH[1] it is shown that the forcing increment  $\Delta F$ , caused by a small increase,  $\Delta \hat{N}^{(i)}$ , in the column density of a greenhouse gas of type  $i$  is

$$\Delta F^{(i)} = P^{(i)} \Delta \hat{N}^{(i)}. \quad (10)$$

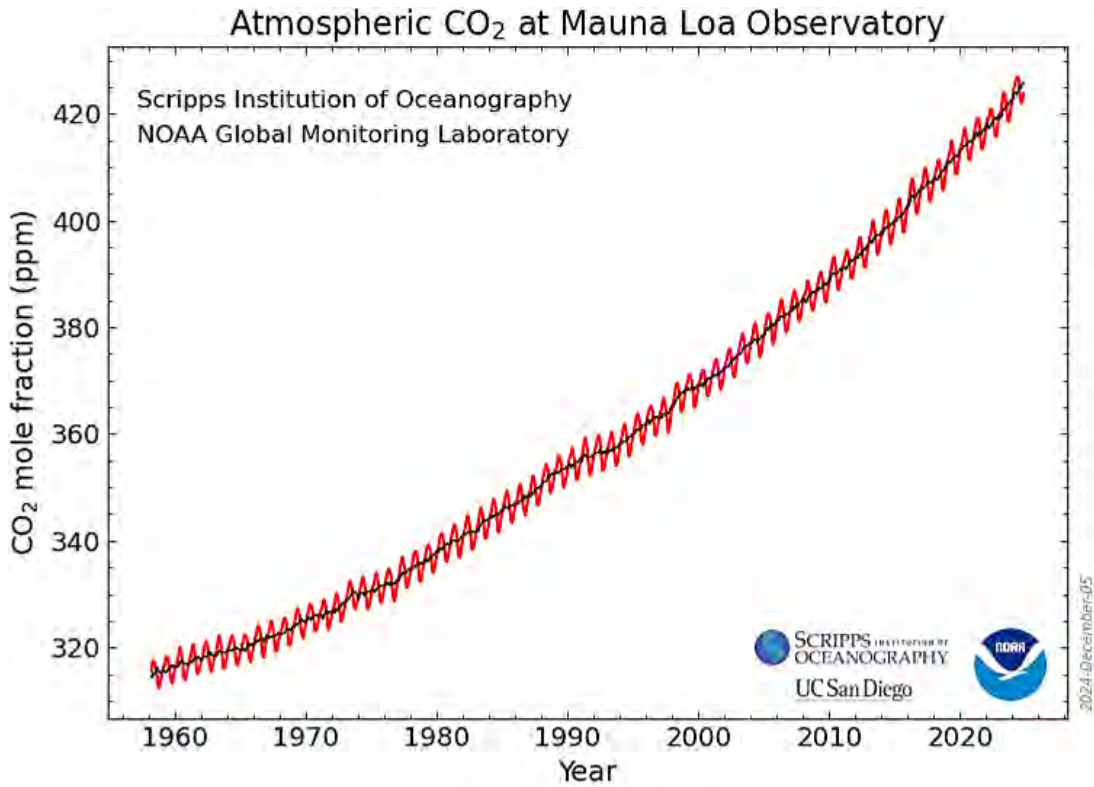


**Figure 8:** Atmospheric concentrations  $\bar{C}^{(i)}$  of carbon dioxide ( $i = \text{CO}_2$ ) molecules versus time [20]. For the past 10 years, the rate of increase has been about  $d\bar{C}^{(i)}/dt = 2.3$  ppm/year.

The column density of the greenhouse gas is determined from the concentrations,  $C^{(i)}(z)$  and total atmospheric number density  $N(z)$  (like those of Fig. 2) by the equation

$$\hat{N}^{(i)} = \int_0^{\infty} C^{(i)} N dz = \bar{C}^{(i)} \hat{N}. \quad (11)$$

Here  $\bar{C}^{(i)}$  is the altitude-averaged concentration of the greenhouse gas, and the column density of all atmospheric molecules is



$$\hat{N} = \int_0^{\infty} N dz = 2.15 \times 10^{29} \text{ m}^{-2}. \quad (12)$$

For the tropopause, WH[1] show that for current atmospheric concentrations of greenhouse gases, the forcing power per molecule for CH<sub>4</sub> and CO<sub>2</sub> are

$$P^{(i)} = 2.8 \times 10^{-24} \text{ W}, \quad \text{for } i = \text{CH}_4, \quad (13)$$

$$P^{(i)} = 9.0 \times 10^{-26} \text{ W}, \quad \text{for } i = \text{CO}_2. \quad (14)$$

Assuming that the concentration growth rates  $d\bar{C}^{(i)}/dt$  of Fig. 7 and Fig. 8 remain the same, the forcing after a time  $t$  will be

$$\Delta F^{(i)} = \hat{N} P^{(i)} (d\bar{C}^{(i)}/dt) t. \quad (15)$$

The per-molecule forcings  $P^{(i)}$  of (13) and (14) have been used with the column density  $\hat{N}$  of (12) and the concentration increase rates  $d\bar{C}^{(i)}/dt$ , noted in Fig. 7 and Fig. 8, to evaluate the future forcing (15), which is plotted in Fig. 9. Even after 50 years, the forcing increments from increased concentrations of methane ( $\Delta F = 0.23 \text{ W m}^{-2}$ ), or the roughly ten times larger forcing from increased carbon dioxide ( $\Delta F = 2.2 \text{ W m}^{-2}$ ) are very small compared to the total forcing,  $\Delta F = 137 \text{ W m}^{-2}$ , shown in Fig. 3.

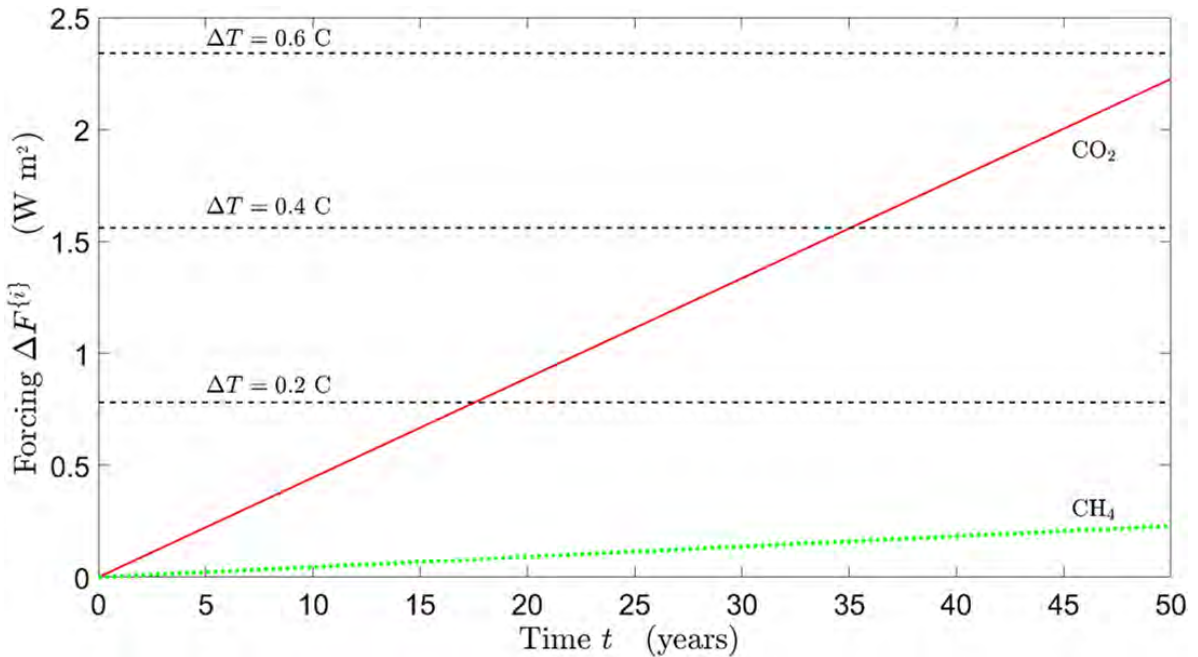


**Figure 9:** Projected midlatitude forcing increments at the tropopause from continued increases of CO<sub>2</sub> and CH<sub>4</sub> at the rates of Fig. 7 and Fig. 8 for the next 50 years. The projected forcings are very small, especially for methane, compared to the current tropospheric forcing of  $137 \text{ W m}^{-2}$ .

Eq. (15) overestimates the forcing changes, which increase more slowly than linearly for large concentration changes. For example, at current concentrations the forcing of CO<sub>2</sub> is proportional to  $\ln(\bar{C}^{(i)})$ , the logarithm of the concentration [22]. But for the concentration changes expected over the next 50 years, the linearized approximation (15) is reasonably accurate.

The reason that the per-molecule forcing of methane is some 30 times larger than that of carbon dioxide for current concentrations is “saturation” of the absorption bands as shown in Fig. 5. The current density of CO<sub>2</sub> molecules is some 200 times greater than that of CH<sub>4</sub> molecules, so the absorption bands of CO<sub>2</sub> are much more saturated than those of CH<sub>4</sub>. In the dilute “optically-thin” limit, WH[1] show that the tropospheric forcing power per molecule is  $P^{(i)} = 0.51 \times 10^{-22}$  W for CH<sub>4</sub>, and  $P^{(i)} = 2.73 \times 10^{-22}$  W for CO<sub>2</sub>. Each CO<sub>2</sub> molecule in the dilute limit causes about five times more forcing increase than an additional molecule of CH<sub>4</sub>, which is only a “super greenhouse gas” because there is so little in the atmosphere, compared to CO<sub>2</sub>.

## ACKNOWLEDGMENTS

### ABOUT THE AUTHORS

#### **Dr. William Happer, CO<sub>2</sub> Coalition Chair, Ph.D. Physics**

Dr. Happer is the Cyrus T. Fogg professor emeritus of physics at Princeton. He is a founder and long-time board member of the CO<sub>2</sub> Coalition. Professor Happer recently returned to the Coalition from a year's government service as Director for Emerging Technologies at the National Security Council. In that position he was also President Trump's adviser on climate science. Professor Happer is perhaps best known for inventing the sodium guide star, which uses ground-based lasers to create an artificial star in the layer of sodium atoms at an altitude of about 90 kilometers. He has published over 200 scientific papers, including those on his pioneering work on the interaction of light and atoms.

#### **Dr. William A. van Wijngaarden, Ph.D. Physics**

Dr. van Wijngaarden is a full professor of physics at York. His research specialties are: high-precision laser spectroscopy, laser cooling and atom trapping, ultracold atoms, Bose-Einstein condensation, pollutant monitoring and climate change.

### EDITOR'S NOTE

This Happer-van Wijngaarden paper is a summary of an extensive paper, *Infrared Forcing of Greenhouse Gases*. Using measurements of hundreds of thousands of individual "line strengths" of the major greenhouse gases in Earth's atmosphere, they show that methane (CH<sub>4</sub>) is nearly irrelevant to global warming. This paper served as the scientific backing for a November 2019 submission to the Environmental Protection Agency by the Life:Powered project of the Texas Public Policy Foundation. The policy implication of the paper is that methane emissions should not be regulated because of any concern about global warming. Cows and pipelines can rest easy.

### ABOUT THE CO<sub>2</sub> COALITION

The CO<sub>2</sub> Coalition was established in 2015 as a non-partisan educational foundation operating under Section 501(c)(3) of the IRS code for the purpose of educating thought leaders, policy makers and the public about the important contribution made by carbon dioxide to our lives and the economy. The Coalition seeks to engage in an informed and dispassionate discussion of climate change, humans' role in the climate system, the limitations of climate models and the consequences of mandated reductions in CO<sub>2</sub> emissions. In carrying out our mission, we seek to strengthen the understanding of the role of science and the scientific process in addressing complex public policy issues like climate change. Science produces empirical, measurable, objective facts and provides a means for testing hypotheses that can be replicated and

potentially disproven. Approaches to policy that do not adhere to the scientific process risk grave damage to the economy and to science.

The Coalition is comprised of more than 160 of the top experts in the world who are skeptical of a theoretical link between increasing CO<sub>2</sub> and a pending climate crisis while embracing the positive aspects of modest warming and increasing CO<sub>2</sub>. They include physicists, chemists, engineers, geologists, economists and more. More than 70% of the members hold doctorates or commensurate degrees and include three members of the National Academy of Sciences.

## REFERENCES

- [1] van Wijngaarden WA, Happer W (2020) Dependence of Earth's Thermal Radiation on Five Most Abundant Greenhouse Gases, Atmospheric and Oceanic Physics, [arXiv:2006.03098](https://arxiv.org/abs/2006.03098)
- [2] Natural gas, <https://www.uniongas.com/about-us/about-natural-gas/chemical-composition-of-natural-gas>
- [3] Methane from coal, <https://www.clarke-energy.com/coal-gas/>
- [4] Marsh gas, [https://link.springer.com/referenceworkentry/10.1007%2F1-4020-4494-1\\_217](https://link.springer.com/referenceworkentry/10.1007%2F1-4020-4494-1_217)
- [5] Methane hydrates, <https://geology.com/articles/methane-hydrates/>
- [6] Digestive system of ruminants, <https://extension.umn.edu/dairy-nutrition/ruminant-digestive-system>
- [7] Sanderson MG (1996) *Biomass of termites and their emissions of methane and carbon dioxide: A global database*, Global Biogeochemical Cycles 10, 543–557, DOI: <https://doi.org/10.1029/96GB01893>
- [8] Methane atmospheric lifetime, [https://gml.noaa.gov/ccgg/trends\\_ch4/](https://gml.noaa.gov/ccgg/trends_ch4/)
- [9] The U.S. Standard Atmosphere, NASA, <https://ntrs.nasa.gov/archive/nasa/casi.ntrs.nasa.gov/19770009539.pdf>.
- [10] Anderson GP, Clough SA, Kneizys FX, Chetwynd JH, Shettle EP (1986) AFGL Atmospheric Constituent Profiles (0–120 km), AFGL-TR-86-0110, [https://www.researchgate.net/publication/235054307\\_AFGL\\_Atmospheric\\_Constituent\\_Profiles\\_0120km#fullTextFileContent](https://www.researchgate.net/publication/235054307_AFGL_Atmospheric_Constituent_Profiles_0120km#fullTextFileContent)
- [11] National Weather Service, Radiosondes or Weather Balloons, <https://www.weather.gov/rah/virtualtourballoon>
- [12] Petty GW (2008) *A First Course in Atmospheric Thermodynamics*, Sundog Publishing, Madison, Wisconsin
- [13] Buoyancy and atmospheric stability, <https://kestrel.nmt.edu/~raymond/classes/ph332/notes/oldstuff/convection/convection.pdf>
- [14] Solar spectrum, <https://www.sciencedirect.com/topics/engineering/solar-spectra>
- [15] Radiative Forcing IPCC, Anthropogenic and Natural Radiative Forcing, [https://www.ipcc.ch/site/assets/uploads/2018/02/WG1AR5\\_Chapter08\\_FINAL.pdf](https://www.ipcc.ch/site/assets/uploads/2018/02/WG1AR5_Chapter08_FINAL.pdf)

- [16] The Planck spectral intensity, [https://en.wikipedia.org/wiki/Planck%27s\\_law](https://en.wikipedia.org/wiki/Planck%27s_law)
- [17] Lambertian intensity distributions,  
<https://omlc.org/classroom/ece532/class1/lambertian.html>
- [18] Fyfe JC, Gillett NP, Zwiers FW (2013) Overestimated global warming over the past 20 years, Nature Climate Change 3, 767–769, DOI: <https://doi.org/10.1038/nclimate1972>
- [19] Manabe S, Wetherald RT (1967) Thermal Equilibrium of the Atmosphere with a Given Distribution of Relative Humidity, Journal of the Atmospheric Sciences 24 (3), 241–259, DOI: [https://doi.org/10.1175/1520-0469\(1967\)024%3C0241:TEOTAW%3E2.0.CO;2](https://doi.org/10.1175/1520-0469(1967)024%3C0241:TEOTAW%3E2.0.CO;2)
- [20] Carbon dioxide concentrations versus time, <https://gml.noaa.gov/ccgg/trends/>
- [21] Charles Keeling’s CO<sub>2</sub> Observatories,  
<https://scripps.ucsd.edu/programs/keelingcurve/>
- [22] Wilson DJ, Gea-Banacloche J (2012) Simple model to estimate the contribution of atmospheric CO<sub>2</sub> to the Earth’s greenhouse effect, American Journal of Physics 80, 306–315, DOI: <https://doi.org/10.1119/1.3681188>